



AVACS – Automatic Verification and Analysis of Complex Systems

REPORTS

of SFB/TR 14 AVACS

Editors: Board of SFB/TR 14 AVACS

AVACS H1/2 8-year Benchmark: Analyzing Traffic Models With iSAT

by

Nam Thang Dinh Martin Fränzle Andreas Eggers

Publisher: Sonderforschungsbereich/Transregio 14 AVACS
(Automatic Verification and Analysis of Complex Systems)
Editors: Bernd Becker, Werner Damm, Bernd Finkbeiner, Martin Fränzle,
Ernst-Rüdiger Olderog, Andreas Podelski
ATRs (AVACS Technical Reports) are freely downloadable from www.avacs.org

AVACS H1/2 8-year Benchmark: Analyzing Traffic Models With iSAT

Nam Thang Dinh, Martin Fränzle, and Andreas Eggers

Carl von Ossietzky Universität, Oldenburg, Germany
{nam.thang.dinh|fraenzle|eggerts}@informatik.uni-oldenburg.de

Abstract. In this technical report, we present an application of the iSAT constraint solver to instances of traffic flow networks. We give an account of the underlying model and provide details of different instances of the model and a variety of verification and falsification tasks handled by our solver.

1 Introduction

Engineers have been interested in modeling, analyzing, and optimizing traffic flows in urban road networks nearly since the beginnings of the automobile. It was as early as the 1930s, when it was discovered that traffic densities in western metropolises had reached levels where their behavior resembled that of pressurized gases [3]. Subsequently, macroscopic models were developed that reflected this observation. While a straight-forward (microscopic) approach is based on modeling e.g. position, speed, and acceleration of individual vehicles, such macroscopic models are developed around smoothed traffic densities—effectively blurring individual behavior of the vehicles. Based on the behavior of (compressible) gases [5] or on that of (incompressible) fluids [4], the dynamics is normally modelled by partial differential equations.

The goal of this report is to show the application of our constraint solver iSAT [2] to instances of such traffic networks. Since iSAT itself does not support partial differential equations that would be needed for a direct representation of such models, we have built an approximation by discretizing space into cells and time into equidistant steps, retaining however the underlying modelling paradigm of *piecewise continuous mass flow equations* governing a *continuous amount of traffic* in each of the cells and hence the lumping of individual cars into a traffic mass that it incorporates.

In Section 2 we detail our modeling approach. Subsequently, Section 3 reports our benchmarking results for different instances of the model. We finally analyze these results in Section 4. For a detailed account of the algorithmic core of iSAT, we refer to [2], and for an overview of the input language, please see the iSAT Quick Start Guide¹. The iSAT solver is available online².

2 Cell-Transition Model

The central building block of our model is the *cell* representing a piece of road. The length of this road (in terms of transfer time under ideal conditions, not geometric length) is characterized by the number of *subcells* in the cell. Subcells are traversed within one time step each — linearly from the beginning of the cell towards its end. The capacity of the road, representing both its width and geometric length, is given by a parameter. Capacities are assigned to cells, whereas subcells do not carry individual capacities, making it possible for the entire amount of traffic in a cell to be distributed arbitrarily over the subcells.

Cells may have an arbitrary number of predecessors and successors. The last subcell of a cell is connected to each of the first subcells of these successors. The outflow of traffic from the last subcell depends on the weights associated with the connections, representing the distribution of

¹ <http://isat.gforge.avacs.org/documentation/quickstartguide.pdf>

² <http://isat.gforge.avacs.org>

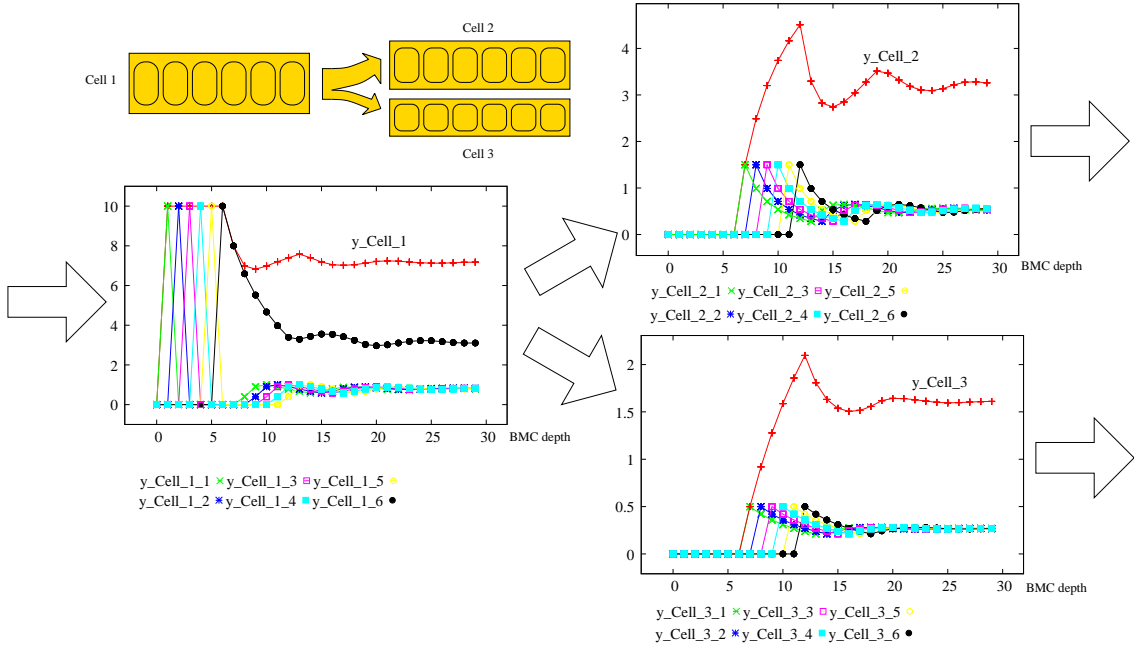


Fig. 1. Trace for the simple model shown in Fig. 2. For each cell, the total traffic density and the distribution to its — in this case — 6 subcells are plotted. In this model, traffic flows from cell 1 to cells 2 and 3, with a weight of 75% on the transmission to cell 2 and 25% on that to cell 3. The initial state is set to zero for all subcells, i.e. all streets start empty. Since the first cell can accept 10 cars in total and the inflow rate is set to 10 cars per time unit, the first cell is filled within the first time unit, blocking further inflow. Outflow does not arise immediately; instead, traffic has to propagate through the subcells until reaching the end of cell 1 from where on it is distributed to the successor cells. Only after the first cars have left cell 1, new inflow can be accommodated, leading to some oscillation which eventually stabilizes to a near-steady state.

the outflow to the successors. Additionally, it is influenced by a dampening behavior such that the actual amount of traffic flowing from cell A to cell B also depends on the degree of saturation of cell B with traffic residing there. While a nearly empty cell B does not hinder traffic significantly from flowing from A , a nearly full cell B lets only small amounts of traffic in. This dampening reflects that traffic slows down when the road ahead is congested. For the purpose of this model, we have not based this dampening on actual empirical data. Instead, we use the following relationship:

$$f_{A \rightarrow B} \leq r_{A \rightarrow B} \cdot (1 - x_B)^2,$$

where $f_{A \rightarrow B}$ is the actual flow from A to B , $r_{A \rightarrow B}$ is the maximum allowed flow rate from A to B , and x_B is cell B 's relative degree of saturation, i.e. the quotient y_B/kp_B , with y_B being the absolute amount of traffic currently residing in road segment B and kp_B the maximum capacity of that road segment.

A very simple instance of this model is given in Figures 1 and 2. From cell 1, traffic flows into the successor cells 2 and 3, with a distribution under free-flowing condition of 3 : 1. Figure 2 shows a predicative encoding of the model using the iSAT input language. Since the initial condition is fixed for this model and there are no nondeterministic choices, there exists only one solution which can be found by iSAT using mere propagation. This trajectory is depicted in Fig. 1. Note that numerical inaccuracies cause widening of this enclosure over time, i.e. later variable instances of the bounded model checking formula get wider valuations due to accumulated rounding errors that have to be captured by the safe interval enclosure. This effect can be clearly seen from the graphs in Fig. 3, which shows the solution for the same model with an unwinding depth of 80 using es exact as possible propagation (no cut-off of propagations with small progress), but no splitting.

```

DECL
-- Maximum capacities of cells.
define kp_C_1 = 10.0; define kp_C_2 = 8.0; define kp_C_3 = 6.0;
-- Maximum traffic flows between cells.
define r_C_1_C_2 = 1.5; define r_C_1_C_3 = 0.5;
-- Maximum outflow of last cells.
define r_C_2_0 = 3.0; define r_C_3_0 = 1.0;
-- Maximum inflow into first cell.
define r0 = 10.0;
-- Distribution of traffic 1->(2,3).
define ratio_C_1_C_2 = 0.75;
define ratio_C_1_C_3 = 0.25;
-- Relative amount of traffic in cells.
float [0,1] x_C_1; float [0,1] x_C_2; float [0,1] x_C_3;
-- Absolute total amount of traffic in cells.
float [0, kp_C_1] y_C_1; float [0, kp_C_2] y_C_2; float [0, kp_C_3] y_C_3;
-- Absolute amount of traffic in subcells.
float [0, kp_C_1] y_C_1_1; float [0, kp_C_2] y_C_1_2; float [0, kp_C_3] y_C_1_3;
float [0, kp_C_1] y_C_1_2; float [0, kp_C_2] y_C_1_3; float [0, kp_C_3] y_C_1_4;
float [0, kp_C_1] y_C_1_3; float [0, kp_C_2] y_C_1_4; float [0, kp_C_3] y_C_1_5;
float [0, kp_C_1] y_C_1_4; float [0, kp_C_2] y_C_1_5; float [0, kp_C_3] y_C_1_6;
float [0, kp_C_1] y_C_1_5; float [0, kp_C_2] y_C_1_6; float [0, kp_C_3] y_C_1_7;
float [0, kp_C_1] y_C_1_6; float [0, kp_C_2] y_C_1_7; float [0, kp_C_3] y_C_1_8;
-- Actual traffic flow into, between, and out of the cells.
float [0, r_C_1_C_2] traffic_flow_C_1_C_2 ;
float [0, r_C_1_C_3] traffic_flow_C_1_C_3 ;
float [0, r0] traffic_flow_0_C_1 ;
float [0, r_C_2_0] traffic_flow_C_2_0 ;
float [0, r_C_3_0] traffic_flow_C_3_0 ;

INIT
-- Initially, all cells empty.
x_C_1 = 0.0; x_C_2 = 0.0; x_C_3 = 0.0; y_C_1 = 0.0; y_C_2 = 0.0; y_C_3 = 0.0;
y_C_1_1 = 0.0; y_C_1_2 = 0.0; y_C_1_3 = 0.0; y_C_1_4 = 0.0; y_C_1_5 = 0.0; y_C_1_6 = 0.0;
y_C_2_1 = 0.0; y_C_2_2 = 0.0; y_C_2_3 = 0.0; y_C_2_4 = 0.0; y_C_2_5 = 0.0; y_C_2_6 = 0.0;
y_C_3_1 = 0.0; y_C_3_2 = 0.0; y_C_3_3 = 0.0; y_C_3_4 = 0.0; y_C_3_5 = 0.0; y_C_3_6 = 0.0;

TRANS
-- Calculate relative from absolute values.
kp_C_1 * x_C_1' = y_C_1'; kp_C_2 * x_C_2' = y_C_2'; kp_C_3 * x_C_3' = y_C_3';
-- Summarize traffic to total amounts.
y_C_1' = y_C_1_1' + y_C_1_2' + y_C_1_3' + y_C_1_4' + y_C_1_5' + y_C_1_6';
y_C_2' = y_C_2_1' + y_C_2_2' + y_C_2_3' + y_C_2_4' + y_C_2_5' + y_C_2_6';
y_C_3' = y_C_3_1' + y_C_3_2' + y_C_3_3' + y_C_3_4' + y_C_3_5' + y_C_3_6';
-- Calculate successor states: Traffic moves to next subcell.
y_C_1_1' = traffic_flow_0_C_1 ;
y_C_1_2' = y_C_1_1; y_C_1_3' = y_C_1_2; y_C_1_4' = y_C_1_3; y_C_1_5' = y_C_1_4;
y_C_1_6' = y_C_1_5 + y_C_1_6 - traffic_flow_C_1_C_2 - traffic_flow_C_1_C_3;
y_C_2_1' = traffic_flow_C_1_C_2 ;
y_C_2_2' = y_C_2_1; y_C_2_3' = y_C_2_2; y_C_2_4' = y_C_2_3; y_C_2_5' = y_C_2_4;
y_C_2_6' = y_C_2_5 + y_C_2_6 - traffic_flow_C_2_0;
y_C_3_1' = traffic_flow_C_1_C_3 ;
y_C_3_2' = y_C_3_1; y_C_3_3' = y_C_3_2; y_C_3_4' = y_C_3_3; y_C_3_5' = y_C_3_4;
y_C_3_6' = y_C_3_5 + y_C_3_6 - traffic_flow_C_3_0;
-- Calculate actual traffic flow, dampening behavior depending on traffic density
-- in successor cells, distribution depending on given weights.
traffic_flow_0_C_1 = min((r0 * (1 - x_C_1)^2), (kp_C_1 - y_C_1));
traffic_flow_C_1_C_2 = min(r_C_1_C_2 * (1 - x_C_2)^2,
                           min((kp_C_2 - y_C_2) * ratio_C_1_C_2, y_C_1_6 * ratio_C_1_C_2));
traffic_flow_C_1_C_3 = min(r_C_1_C_3 * (1 - x_C_3)^2,
                           min((kp_C_3 - y_C_3) * ratio_C_1_C_3, y_C_1_6 * ratio_C_1_C_3));
traffic_flow_C_2_0 = min(r_C_2_0, y_C_2_6);
traffic_flow_C_3_0 = min(r_C_3_0, y_C_3_6);

TARGET
-- No particular target state. Setting minimum number of unwindings from outside.
true;

```

Fig. 2. Input model for three-cell basic instance.

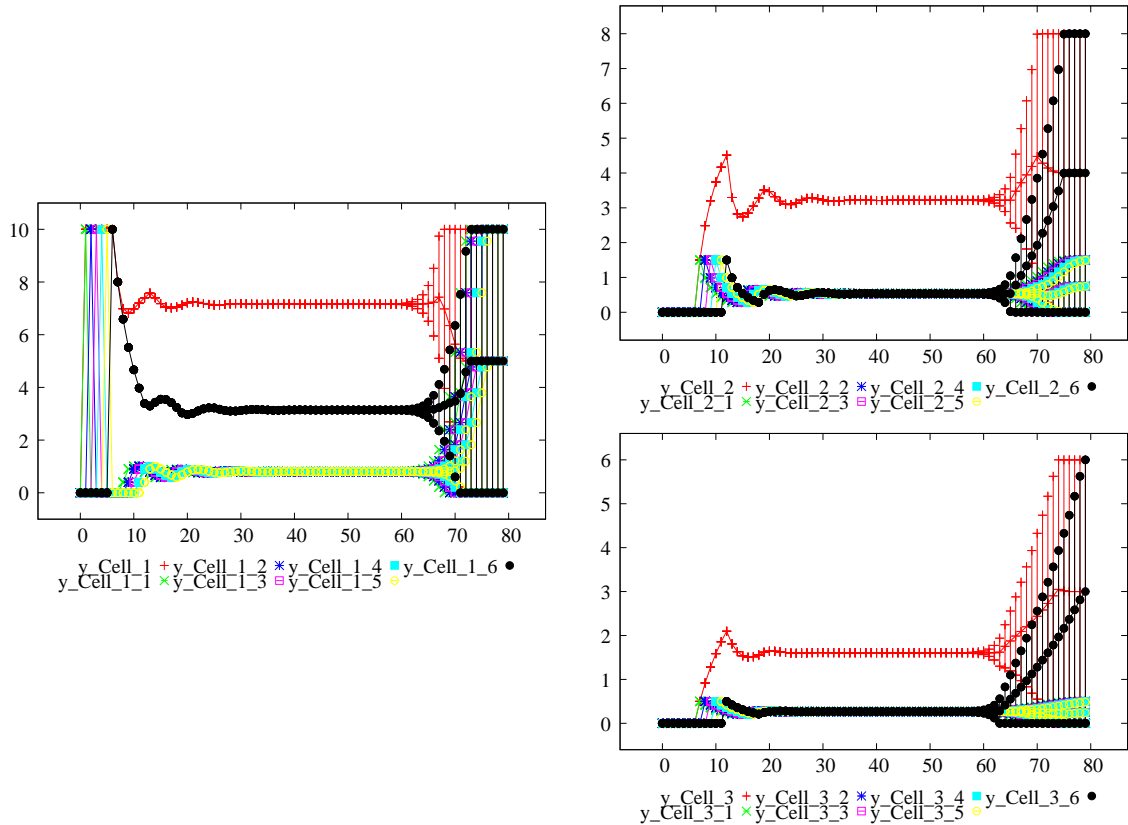


Fig. 3. Propagation-only (i.e., pure interval constraint propagation, decision steps in iSAT disabled) result for the model depicted in Fig. 2. The width of the safe trajectory enclosure diverges until eventually entire variable domains are covered, i.e. propagation alone becomes too weak to find the solution trajectory since accumulated numerical inaccuracies become too big. As this divergence is due to safe rounding, it proves that obtaining valid trajectories for this model via numerical simulation is far from straightforward.

Using iSAT with splitting enabled, candidate solutions with tight interval widths can be found in these cases, however at significantly higher computational cost than is to be expected in a situation where only one solution exists that is in principle obtainable by mere forward propagation from the point-valued initial state. The effect could be controlled by using higher precision data types for the variables. However, since this has not been done to accomodate this special case, this issue has to be kept in mind when using iSAT for actual model checking queries in which equally long propagation chains might occur. Some of the experiments below make use of this observation by explicitly aiming at verification goals that do not require such large unwindings.

To simplify the modeling of larger road networks, we have built a small JAVA tool that compiles a high-level description (given as parameterized cell objects and connections) of a road network into the format shown in Fig. 2. Manual steps are thus confined to modifying the resulting model, e.g. by adding target conditions or more relaxed initial constraints. This approach reduces the potential for modeling errors which may easily arise when creating models of more complex road networks by hand.

3 Experiments

In the following, we describe the application of the iSAT algorithm to different instances of the model described in the previous section. Runtimes are reported for the experiments on AMD Opteron 8378 processors at 2.4 GHz running 64 bit Linux. We have limited memory consumption to 4 GiB per

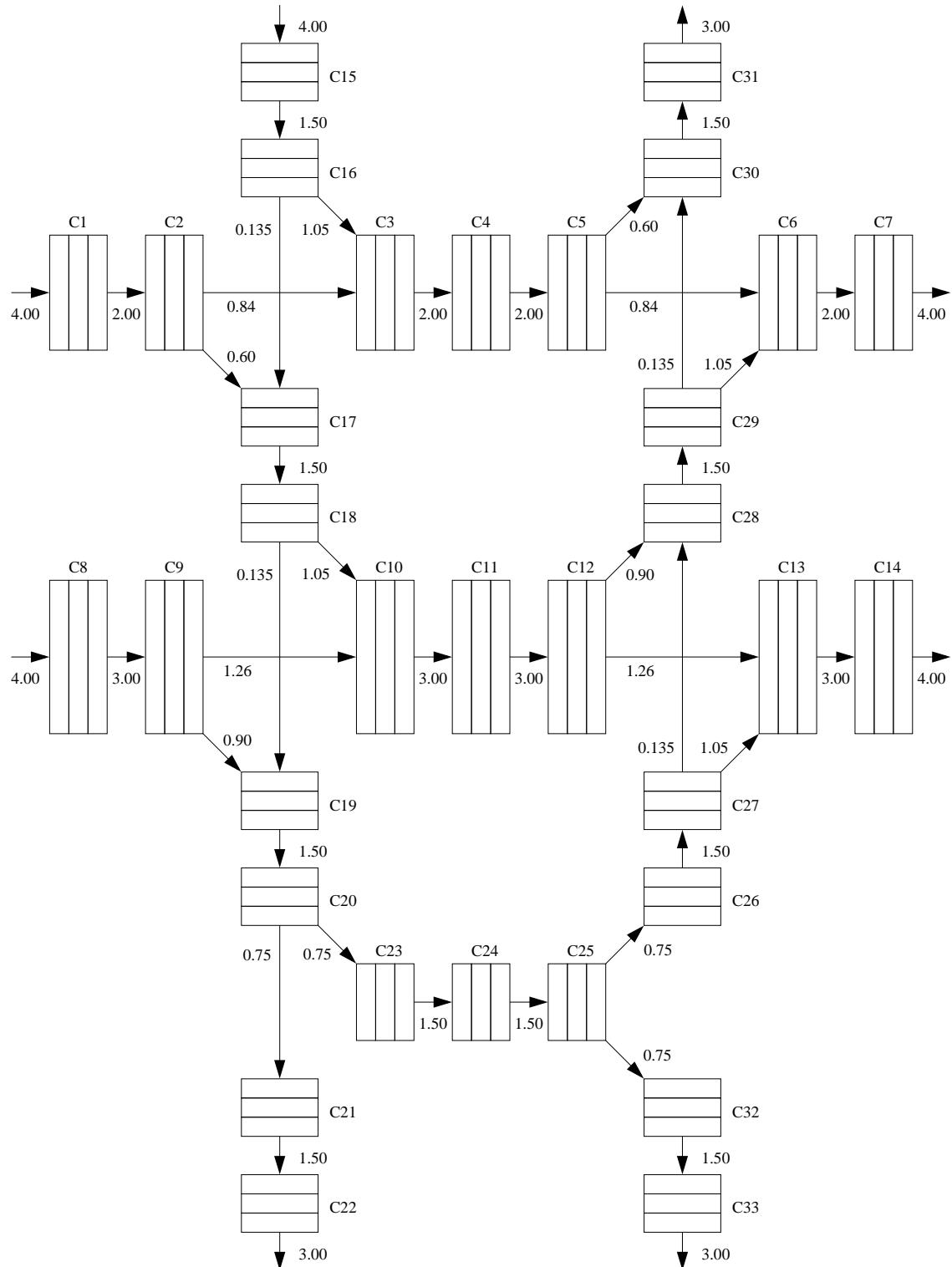


Fig. 4. Complex road network. All cells have three subcells. Cells 1 to 7 have capacity 6, cells 8 to 15 have capacity 8, while all other cells have capacity 4. Arrows represent possible transfer of traffic between cells, with the maximum permitted flow rates affixed to the arrows. Note that the actual flow rates are subject to dampening caused by congestion in the target cells and availability of cars in the source cells. At the borders of the network, inflowing traffic is always available up to the given maximum rate of 4.00 and outflowing traffic can always be absorbed up to the given rates.

solver process and set a time limit of 10000 seconds of CPU time per process. We compare four different implementations of the iSAT algorithm:

- the latest version of the original implementation **hysat-0.8.6** (in the AVACS proposal, this version is called HySAT II, the suffix 0.8.6 is an internal version number used here for ensuring reproducibility of results),
- the first official release of its reimplementation **isat_1.0r1322**,
- a more recent development version of iSAT, called **isat_r2117**, and
- a version employing different rewriting mechanisms in its frontend, originally intended to mitigate restrictions on the size of rational constants and better detection of potential overflows, called **isat_sf_r2117**.

For the evaluation, we use different settings for the *minimum splitting width* ($\text{msw} \in \{0.1, 0.01, 0.001\}$), i.e. the threshold under which interval boxes that are found to be consistent are not split further, and the *absolute bound progress / minimum bound delta* ($\text{prabs} \in \{0.01, 0.001, 0.0001\}$), i.e. the threshold under which newly deduced bounds are discarded to limit the length of implication chains. We disregard the unreasonable combinations of settings where $\text{prabs} \geq \text{msw}$, which are not supported by iSAT and can cause problems with HySAT. For the splitting heuristics, we only use the respective default heuristics. Note, however, that different choices may have significant effects on solver runtimes.

3.1 Finding fixed points for road networks (1_fixed_points)

The first experiment is to let our solver find fixed points of the transition system representing the road network depicted in Fig. 4. By adding, for all variables $y_{i,j}$ describing the amount of traffic in subcell j of cell i , the constraint $y'_{i,j} = y_{i,j}$, i.e. demanding that the post-value $y'_{i,j}$ equals the pre-value $y_{i,j}$ the resulting formula is only satisfied by valuations that represent a fixed-point with respect to the original transition system. Table 1 lists results and runtimes for this benchmark. To illustrate the solver output, Table 2 displays the amount of traffic in each of the subcells of the road network from Fig. 4.

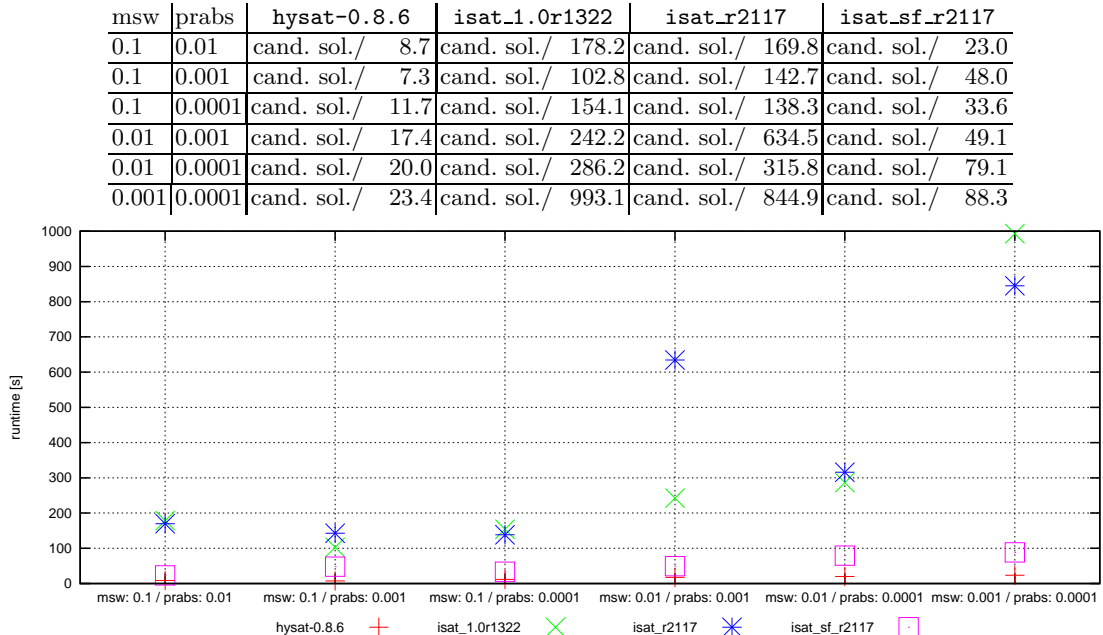


Table 1. Results and runtimes in seconds for finding fixed points in the large road network from Fig. 4. Input files and raw solver outputs are filed under the label **1_fixed_points** in the accompanying archive.

cell	amount of traffic	cell	amount of traffic	cell	amount of traffic
1	[3.63554397,3.63633198]	12	[2.64737445,2.64790956]	23	[0.67839403,0.67903125]
1_1	[0.62076961,0.62118359]	12_1	[0.88212327,0.8826591)	23_1	(0.22570926,0.22614049)
1_2	[0.62076961,0.62118359]	12_2	[0.88212327,0.88269115]	23_2	(0.22570926,0.22614049)
1_3	[2.39359077,2.39409183]	12_3	[0.88262559,0.88312791]	23_3	(0.22602378,0.22675028)
2	(2.65614087,2.6567305)	13	[2.09046815,2.09129416]	24	[0.67943579,0.68002127)
2_1	(0.62096949,0.62128164)	13_1	[0.69670955,0.69730843)	24_1	(0.22602378,0.22653272)
2_2	(0.62096949,0.62128164)	13_2	[0.69670955,0.69730843)	24_2	(0.22602378,0.22653272)
2_3	[1.41391668,1.41450631)	13_3	[0.6968793,0.69750329)	24_3	[0.22641326,0.22695585)
3	[2.33601402,2.33654059]	14	[2.09173751,2.09246459]	25	[0.67957211,0.68024783)
3_1	(0.70450907,0.70480165]	14_1	[0.6968793,0.69750329)	25_1	[0.22641326,0.22682276]
3_2	(0.70450907,0.70480165]	14_2	[0.6968793,0.69750329)	25_2	[0.22641326,0.22682276]
3_3	[0.92641073,0.92722987)	14_3	[0.6974291,0.69818508)	25_3	[0.22606986,0.2267411)
4	[2.43748076,2.43805333]	15	[2.64085999,2.64171224]	26	[0.33903363,0.33984201)
4_1	[0.70485911,0.70508574]	15_1	[0.46101244,0.46167513]	26_1	[0.11303493,0.11331343)
4_2	[0.70485911,0.70508574]	15_2	[0.46101244,0.46167513]	26_2	[0.11303493,0.1132186)
4_3	[1.0275359,1.02833509]	15_3	[1.71836198,1.71902467)	26_3	[0.11296376,0.11347134]
5	[2.43790107,2.43833801]	16	(1.78166355,1.78244257)	27	[0.33869478,0.33934147]
5_1	[0.70474645,0.70491938]	16_1	[0.4608877,0.46134531)	27_1	[0.11296376,0.11305725]
5_2	[0.70474645,0.70491938]	16_2	[0.4608877,0.46134531)	27_2	[0.11296376,0.11305725]
5_3	[1.02840817,1.02884511]	16_3	(0.8593974,0.86020956]	27_3	[0.11267377,0.11318073)
6	[1.87818356,1.87885031]	17	(1.13277765,1.13309579)	28	[0.896232,0.8970259)
6_1	[0.62593411,0.6264081]	17_1	(0.37747094,0.37771094)	28_1	[0.29868018,0.2988926)
6_2	[0.62593411,0.6264081]	17_2	(0.37747094,0.37771094)	28_2	[0.29868018,0.2988926)
6_3	[0.62612472,0.62670087)	17_3	(0.37735577,0.37784522)	28_3	(0.29865922,0.29921868)
7	[1.87880061,1.87956042]	18	(1.39288955,1.39336791]	29	[0.92602055,0.92672304)
7_1	[0.62612472,0.62670087)	18_1	(0.37735577,0.37791413)	29_1	(0.29865922,0.29921868)
7_2	[0.62613345,0.62670087)	18_2	(0.37735577,0.37791413)	29_2	(0.29865922,0.29921868)
7_3	[0.62633794,0.62691848]	18_3	(0.63762458,0.63817306]	29_3	[0.32787923,0.32855635]
8	[4.08747935,4.08821832)	19	(1.35613542,1.35662699)	30	(1.13241414,1.13318247)
8_1	(0.95637724,0.95698408)	19_1	(0.45188751,0.45228227)	30_1	(0.37743698,0.37773859)
8_2	(0.95637724,0.95698408)	19_2	(0.45188751,0.45228227)	30_2	(0.37743698,0.37773859)
8_3	(2.17361205,2.17435102)	19_3	(0.45189228,0.4523579)	30_3	(0.37717721,0.37774276)
9	[3.48197076,3.4825836]	20	(1.35532991,1.35606553]	31	(1.13160575,1.13225799)
9_1	(0.95653523,0.95688323]	20_1	(0.45189228,0.4523579)	31_1	(0.37717721,0.37774276)
9_2	(0.95653523,0.95688323]	20_2	(0.45189228,0.4523579)	31_2	(0.37717721,0.37774276)
9_3	[1.5682043,1.56888963)	20_3	(0.45154535,0.45228097)	31_3	[0.37725132,0.37790165]
10	[2.64829321,2.64904266)	21	(0.67755267,0.67850423)	32	[0.33943738,0.34025051)
10_1	[0.88265558,0.88289837)	21_1	(0.22570926,0.22614049)	32_1	[0.11303493,0.11337055)
10_2	[0.88265558,0.88289837)	21_2	(0.22570926,0.22614049)	32_2	[0.11303493,0.11337055)
10_3	(0.88249649,0.88345237)	21_3	[0.2259217,0.22644204]	32_3	(0.11269629,0.11351703)
11	(2.64760613,2.64824623]	22	(0.67712999,0.67786332]	33	(0.33768628,0.33844619]
11_1	(0.88249649,0.88313658)	22_1	[0.2259217,0.22592171]	33_1	(0.11269629,0.11351703)
11_2	(0.88249649,0.88306482)	22_2	[0.2259217,0.22592171]	33_2	(0.11269629,0.11351703)
11_3	[0.88212327,0.8826591]	22_3	(0.22528658,0.2260199]	33_3	(0.11225304,0.11304169)

Table 2. Fixed point for the traffic system in Fig. 4 as obtained by `iSAT-1.0r1322` using a minimum splitting width of 0.001 and an absolute bound progress of 0.0001.

As can be seen from Table 1, the solvers report candidate solution boxes (marked *cand. sol.*) for all settings with splitting width strictly greater than absolute bound progress. This result indicates that there is a small box whose maximum width lies below the minimum splitting width and that cannot be refuted by interval constraint propagation.

3.2 Showing absence of further fixed points (2_absence_of_fixed_points)

In a second experiment, we show that the fixed point found in the previous experiment essentially is unique. More precisely, we show that a certain rectangular overapproximation of the candidate solution boxes from the experiment in Sect. 3.1 contains all fixed points of the system. To prove this mechanically, we use iSAT to show that a restricted version of the model, where fixed points are confined to the complement of that overapproximation, becomes unsatisfiable. While the candidate solution boxes from the previous experiment came without a strict guarantee of existence of real-valued solution, such unsatisfiability results are actual certificates (under the assumption of a correct implementation) for the absence of fixed points in these parts of the variable domains.

Table 3 reports the results and runtimes for the extended model. As can be seen, all solver instances have been able to prove unsatisfiability of the formula, hence absence of fixed points in the specified region.

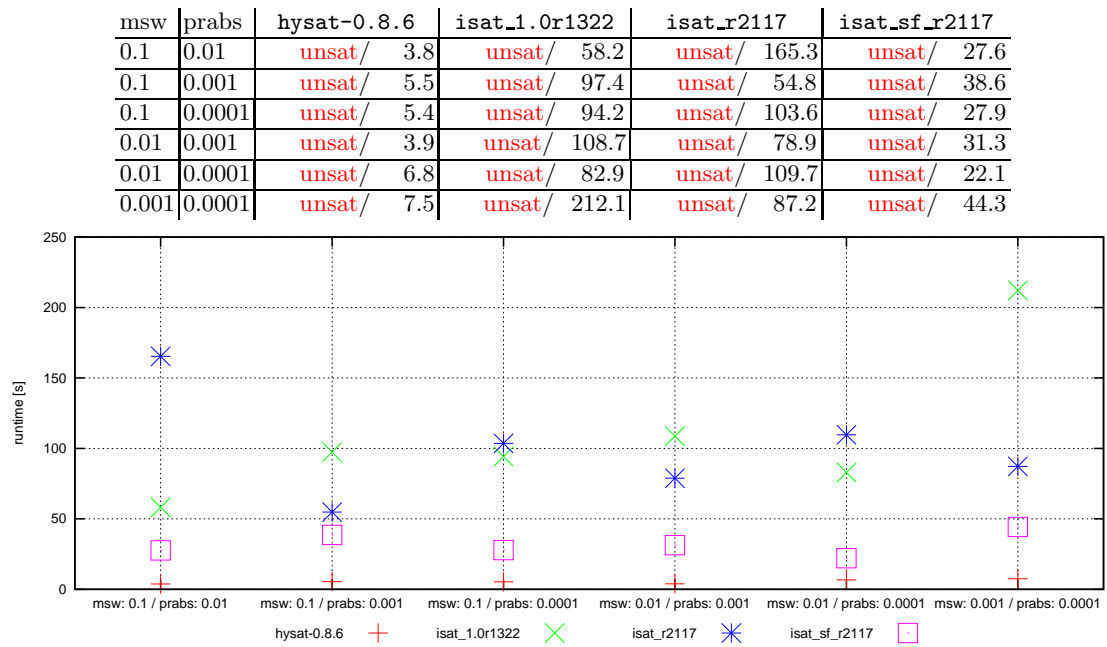


Table 3. Results and runtimes in seconds for showing the absence of fixed points in the large road network from Fig. 4. Input files and raw solver outputs are filed under the label `2_absence_of_points` in the accompanying archive.

3.3 Finding parameters for optimal flow rates (3_finding_parameters)

Aiming at a scenario demonstrating the feasibility of flow optimization by constraint solving, the third experiment addressed automated search for adequate flow rates between cells in the road network. Instead of constants defining the maximum flow rates between cells, variables are introduced into the model and are given a wide range of possible values. The initial predicate is extended to constrain the initial state to any amount of traffic below 20% of the cell capacity.

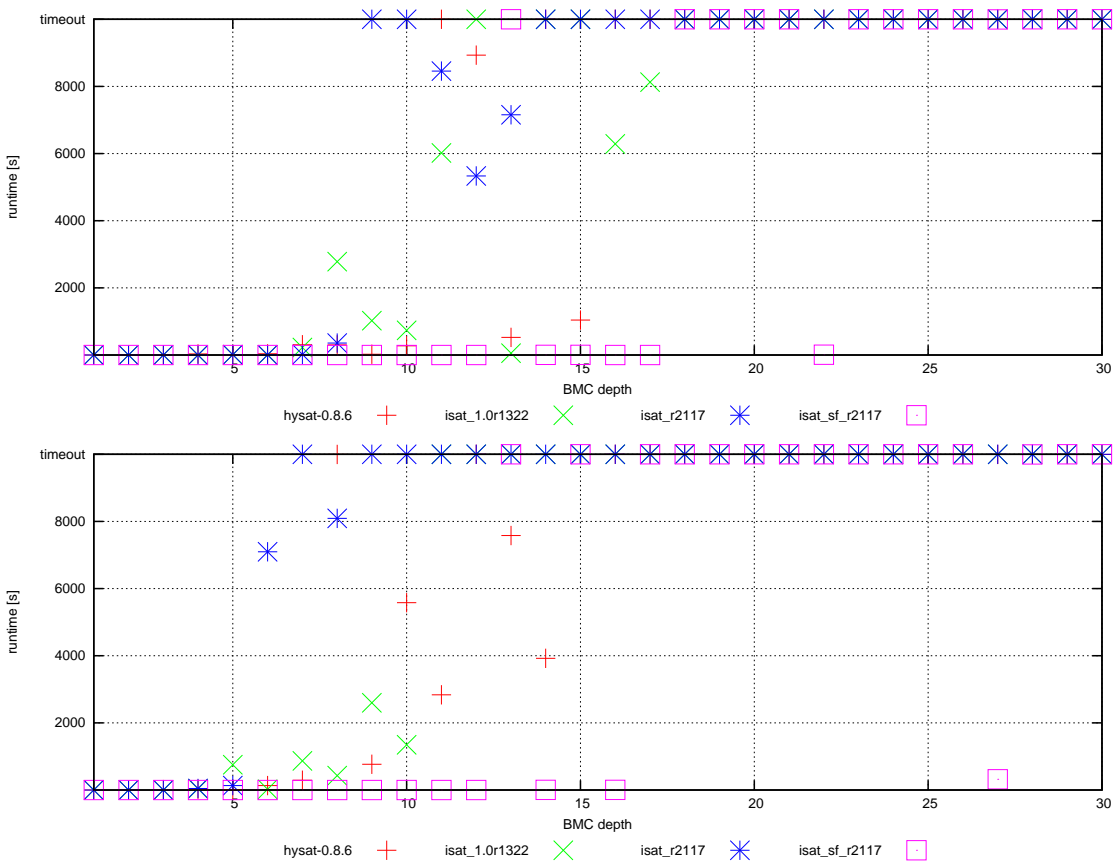


Fig. 5. Runtimes for the `3_finding_parameters` experiment over BMC unwinding depths for the different solver settings. From top to bottom: msw 0.1, prabs: 0.01; msw 0.1, prabs 0.001.

Additionally, the transition predicate is extended such that it becomes false should the amount of traffic rise above 80% in a cell. Thus, a satisfying valuation will contain parameters for the maximum traffic flow rates and instantiated values for the amount of traffic within the cells such that none of the cells reaches an amount of traffic above 80% within the achieved number of formula unwindings. Note that the more general question of whether the found parameters guarantee that all evolutions starting from allowed initial states will stay below 80% degree of filling, requires a quantifier alternation. In the actual scenario, one could check for a found instantiation if there is such a counterexample by modeling this instance explicitly.

Since this benchmark is significantly harder to handle for our solver, we use a small road network, which is a linear road segment of only four cells with three subcells each.

We report results for unwinding depths 1 to 18 in Tables 4 to 21 and illustrate the runtimes for depths 1 to 30 in Figures 5 and 6. For all instances, the solvers either find candidate solutions or are terminated after more than 10000 seconds of CPU time. Timeouts are encountered more often for higher unwinding depths, obviously indicating that these are on average harder to solve. Refined settings (smaller splitting widths and absolute bound progress) make it additionally harder to find candidate solutions — an unsurprising result since larger settings for these parameters may allow spurious solutions that would have to be refuted for the refined settings.

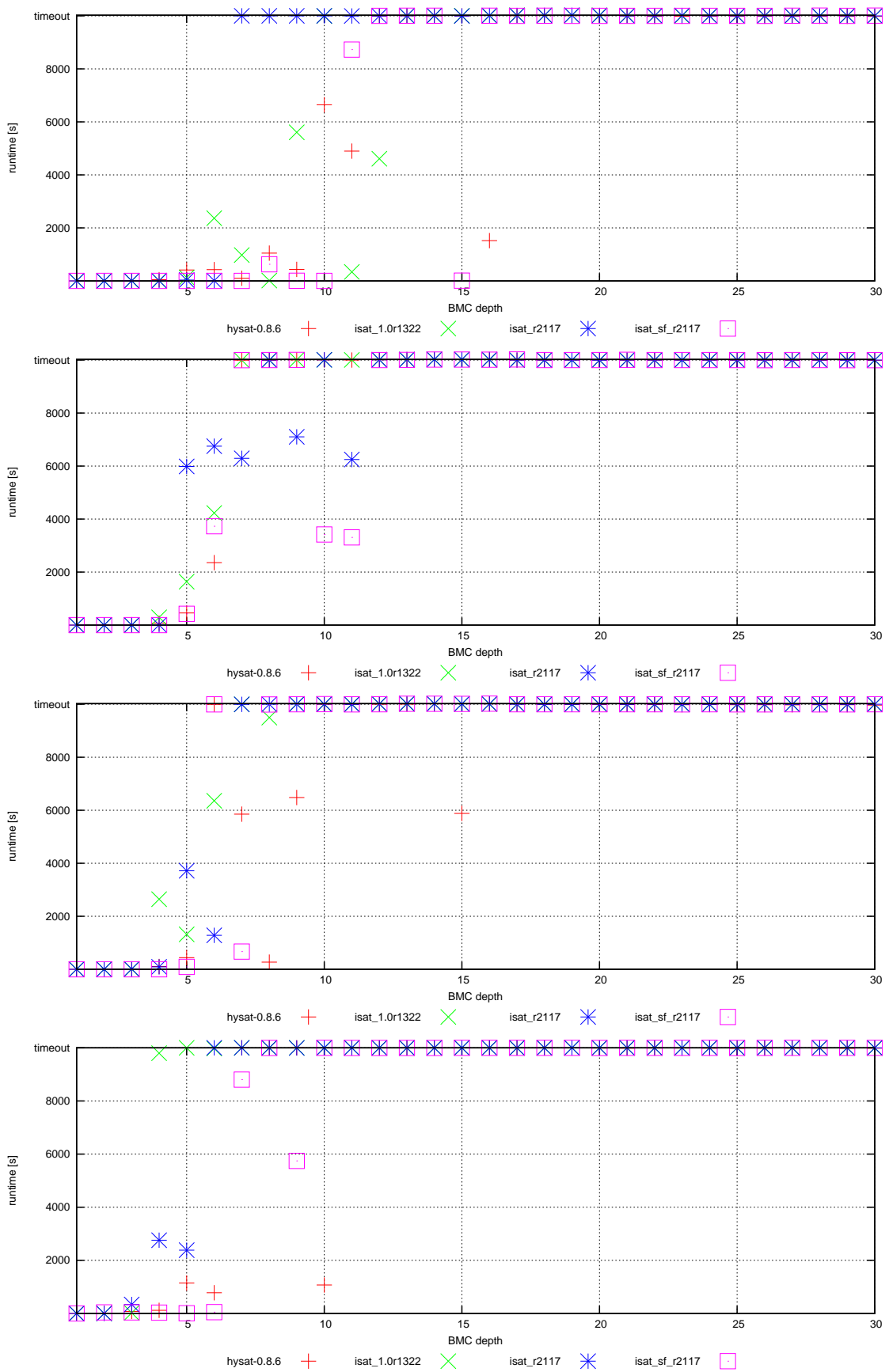


Fig. 6. Runtimes for the `3_finding_parameters` experiment over BMC unwinding depths for the different solver settings. From top to bottom: msw 0.1, prabs 0.0001; msw 0.01, prabs 0.001; msw 0.01, prabs 0.0001; msw 0.001, prabs 0.0001.

msw	prabs	hysat-0.8.6	isat_1.0r1322	isat_r2117	isat_sf_r2117
0.1	0.01	cand. sol./ 0.0	cand. sol./ 0.0	cand. sol./ 0.0	cand. sol./ 0.0
0.1	0.001	cand. sol./ 0.0	cand. sol./ 0.0	cand. sol./ 0.0	cand. sol./ 0.0
0.1	0.0001	cand. sol./ 0.0	cand. sol./ 0.0	cand. sol./ 0.0	cand. sol./ 0.0
0.01	0.001	cand. sol./ 0.7	cand. sol./ 0.0	cand. sol./ 0.0	cand. sol./ 0.1
0.01	0.0001	cand. sol./ 0.3	cand. sol./ 0.0	cand. sol./ 0.0	cand. sol./ 0.1
0.001	0.0001	cand. sol./ 0.3	cand. sol./ 0.1	cand. sol./ 0.0	cand. sol./ 0.1

Table 4. Results and runtimes for finding parameters in the small street network, filed under `3_finding_parameters`, BMC depth 1

msw	prabs	hysat-0.8.6	isat_1.0r1322	isat_r2117	isat_sf_r2117
0.1	0.01	cand. sol./ 0.3	cand. sol./ 0.0	cand. sol./ 0.1	cand. sol./ 0.0
0.1	0.001	cand. sol./ 0.3	cand. sol./ 0.1	cand. sol./ 0.2	cand. sol./ 0.0
0.1	0.0001	cand. sol./ 0.5	cand. sol./ 0.1	cand. sol./ 0.2	cand. sol./ 0.0
0.01	0.001	cand. sol./ 2.5	cand. sol./ 0.1	cand. sol./ 0.1	cand. sol./ 0.2
0.01	0.0001	cand. sol./ 2.0	cand. sol./ 0.2	cand. sol./ 0.2	cand. sol./ 0.7
0.001	0.0001	cand. sol./ 12.4	cand. sol./ 1.3	cand. sol./ 0.9	cand. sol./ 39.6

Table 5. Results and runtimes for `3_finding_parameters`, BMC depth 2

msw	prabs	hysat-0.8.6	isat_1.0r1322	isat_r2117	isat_sf_r2117
0.1	0.01	cand. sol./ 0.9	cand. sol./ 0.1	cand. sol./ 0.7	cand. sol./ 0.0
0.1	0.001	cand. sol./ 11.4	cand. sol./ 1.1	cand. sol./ 1.0	cand. sol./ 0.1
0.1	0.0001	cand. sol./ 3.6	cand. sol./ 0.2	cand. sol./ 3.1	cand. sol./ 0.0
0.01	0.001	cand. sol./ 14.6	cand. sol./ 0.1	cand. sol./ 1.0	cand. sol./ 1.1
0.01	0.0001	cand. sol./ 7.0	cand. sol./ 6.8	cand. sol./ 13.1	cand. sol./ 1.4
0.001	0.0001	cand. sol./ 76.0	cand. sol./ 24.8	cand. sol./ 335.7	cand. sol./ 40.7

Table 6. Results and runtimes for `3_finding_parameters`, BMC depth 3

msw	prabs	hysat-0.8.6	isat_1.0r1322	isat_r2117	isat_sf_r2117
0.1	0.01	cand. sol./ 29.9	cand. sol./ 1.0	cand. sol./ 0.4	cand. sol./ 0.1
0.1	0.001	cand. sol./ 24.2	cand. sol./ 36.8	cand. sol./ 46.5	cand. sol./ 0.1
0.1	0.0001	cand. sol./ 46.7	cand. sol./ 11.1	cand. sol./ 5.6	cand. sol./ 0.1
0.01	0.001	cand. sol./ 74.3	cand. sol./ 290.8	cand. sol./ 4.1	cand. sol./ 0.3
0.01	0.0001	cand. sol./ 104.9	cand. sol./ 2644.2	cand. sol./ 93.8	cand. sol./ 1.2
0.001	0.0001	cand. sol./ 117.2	cand. sol./ 9799.5	cand. sol./ 2757.1	cand. sol./ 34.0

Table 7. Results and runtimes for `3_finding_parameters`, BMC depth 4

msw	prabs	hysat-0.8.6	isat_1.0r1322	isat_r2117	isat_sf_r2117
0.1	0.01	cand. sol./ 6.2	cand. sol./ 7.3	cand. sol./ 8.4	cand. sol./ 0.1
0.1	0.001	cand. sol./ 14.6	cand. sol./ 752.6	cand. sol./ 134.6	cand. sol./ 0.1
0.1	0.0001	cand. sol./ 413.5	cand. sol./ 127.4	cand. sol./ 30.1	cand. sol./ 0.1
0.01	0.001	cand. sol./ 457.0	cand. sol./ 1639.3	cand. sol./ 5984.6	cand. sol./ 424.3
0.01	0.0001	cand. sol./ 437.3	cand. sol./ 1319.4	cand. sol./ 3716.5	cand. sol./ 89.8
0.001	0.0001	cand. sol./ 1147.8	timeout	cand. sol./ 2382.6	cand. sol./ 7.4

Table 8. Results and runtimes for `3_finding_parameters`, BMC depth 5

msw	prabs	hysat-0.8.6	isat_1.0r1322	isat_r2117	isat_sf_r2117
0.1	0.01	cand. sol./ 37.7	cand. sol./ 2.9	cand. sol./ 6.2	cand. sol./ 0.3
0.1	0.001	cand. sol./ 134.0	cand. sol./ 21.7	cand. sol./ 7097.8	cand. sol./ 0.2
0.1	0.0001	cand. sol./ 427.2	cand. sol./ 2365.8	cand. sol./ 7.3	cand. sol./ 0.2
0.01	0.001	cand. sol./ 2354.6	cand. sol./ 4227.8	cand. sol./ 6750.9	cand. sol./ 3730.3
0.01	0.0001	timeout	cand. sol./ 6358.5	cand. sol./ 1283.3	timeout
0.001	0.0001	cand. sol./ 779.8	cand. sol./ 9979.3	timeout	cand. sol./ 48.7

Table 9. Results and runtimes for `3_finding_parameters`, BMC depth 6

msw	prabs	hysat-0.8.6	isat_1.0r1322	isat_r2117	isat_sf_r2117
0.1	0.01	cand. sol./ 305.2	cand. sol./ 223.5	cand. sol./ 16.2	cand. sol./ 0.2
0.1	0.001	cand. sol./ 292.6	cand. sol./ 868.0	timeout	cand. sol./ 0.2
0.1	0.0001	cand. sol./ 102.0	cand. sol./ 972.7	timeout	cand. sol./ 0.2
0.01	0.001	timeout	timeout	cand. sol./ 6290.3	timeout
0.01	0.0001	cand. sol./ 5855.4	timeout	timeout	cand. sol./ 669.2
0.001	0.0001	timeout	timeout	timeout	cand. sol./ 8804.8

Table 10. Results and runtimes for 3_finding_parameters, BMC depth 7

msw	prabs	hysat-0.8.6	isat_1.0r1322	isat_r2117	isat_sf_r2117
0.1	0.01	cand. sol./ 302.4	cand. sol./ 2779.1	cand. sol./ 357.1	cand. sol./ 0.3
0.1	0.001	timeout	cand. sol./ 430.6	cand. sol./ 8090.6	cand. sol./ 0.2
0.1	0.0001	cand. sol./ 1048.3	cand. sol./ 12.3	timeout	cand. sol./ 624.7
0.01	0.001	timeout	timeout	timeout	timeout
0.01	0.0001	cand. sol./ 272.2	cand. sol./ 9495.2	timeout	timeout
0.001	0.0001	timeout	timeout	timeout	timeout

Table 11. Results and runtimes for 3_finding_parameters, BMC depth 8

msw	prabs	hysat-0.8.6	isat_1.0r1322	isat_r2117	isat_sf_r2117
0.1	0.01	cand. sol./ 24.7	cand. sol./ 1021.6	timeout	cand. sol./ 0.3
0.1	0.001	cand. sol./ 766.3	cand. sol./ 2599.9	timeout	cand. sol./ 0.3
0.1	0.0001	cand. sol./ 434.0	cand. sol./ 5605.8	timeout	cand. sol./ 3.0
0.01	0.001	timeout	timeout	cand. sol./ 7099.8	timeout
0.01	0.0001	cand. sol./ 6479.2	timeout	timeout	timeout
0.001	0.0001	timeout	timeout	timeout	cand. sol./ 5746.5

Table 12. Results and runtimes for 3_finding_parameters, BMC depth 9

msw	prabs	hysat-0.8.6	isat_1.0r1322	isat_r2117	isat_sf_r2117
0.1	0.01	cand. sol./ 271.9	cand. sol./ 735.9	timeout	cand. sol./ 0.6
0.1	0.001	cand. sol./ 5579.6	cand. sol./ 1349.2	timeout	cand. sol./ 0.3
0.1	0.0001	cand. sol./ 6643.8	timeout	timeout	cand. sol./ 2.0
0.01	0.001	timeout	timeout	timeout	cand. sol./ 3416.5
0.01	0.0001	timeout	timeout	timeout	timeout
0.001	0.0001	cand. sol./ 1074.6	timeout	timeout	timeout

Table 13. Results and runtimes for 3_finding_parameters, BMC depth 10

msw	prabs	hysat-0.8.6	isat_1.0r1322	isat_r2117	isat_sf_r2117
0.1	0.01	timeout	cand. sol./ 6016.2	cand. sol./ 8454.9	cand. sol./ 0.7
0.1	0.001	cand. sol./ 2836.5	timeout	timeout	cand. sol./ 0.4
0.1	0.0001	cand. sol./ 4897.5	cand. sol./ 337.3	timeout	cand. sol./ 8726.6
0.01	0.001	timeout	timeout	cand. sol./ 6245.1	cand. sol./ 3307.6
0.01	0.0001	timeout	timeout	timeout	timeout
0.001	0.0001	timeout	timeout	timeout	timeout

Table 14. Results and runtimes for 3_finding_parameters, BMC depth 11

msw	prabs	hysat-0.8.6	isat_1.0r1322	isat_r2117	isat_sf_r2117
0.1	0.01	cand. sol./ 8931.9	timeout	cand. sol./ 5335.5	cand. sol./ 1.0
0.1	0.001	timeout	timeout	timeout	cand. sol./ 1.0
0.1	0.0001	timeout	cand. sol./ 4606.5	timeout	timeout
0.01	0.001	timeout	timeout	timeout	timeout
0.01	0.0001	timeout	timeout	timeout	timeout
0.001	0.0001	timeout	timeout	timeout	timeout

Table 15. Results and runtimes for 3_finding_parameters, BMC depth 12

msw	prabs	hysat-0.8.6	isat_1.0r1322	isat_r2117	isat_sf_r2117
0.1	0.01	cand. sol./ 524.7	cand. sol./ 52.8	cand. sol./ 7156.3	timeout
0.1	0.001	cand. sol./ 7580.6	timeout	timeout	timeout
0.1	0.0001	timeout	timeout	timeout	timeout
0.01	0.001	timeout	timeout	timeout	timeout
0.01	0.0001	timeout	timeout	timeout	timeout
0.001	0.0001	timeout	timeout	timeout	timeout

Table 16. Results and runtimes for 3_finding_parameters, BMC depth 13

msw	prabs	hysat-0.8.6	isat_1.0r1322	isat_r2117	isat_sf_r2117
0.1	0.01	timeout	timeout	timeout	cand. sol./ 2.6
0.1	0.001	cand. sol./ 3922.3	timeout	timeout	cand. sol./ 2.5
0.1	0.0001	timeout	timeout	timeout	timeout
0.01	0.001	timeout	timeout	timeout	timeout
0.01	0.0001	timeout	timeout	timeout	timeout
0.001	0.0001	timeout	timeout	timeout	timeout

Table 17. Results and runtimes for 3_finding_parameters, BMC depth 14

msw	prabs	hysat-0.8.6	isat_1.0r1322	isat_r2117	isat_sf_r2117
0.1	0.01	cand. sol./ 1040.5	timeout	timeout	cand. sol./ 2.3
0.1	0.001	timeout	timeout	timeout	timeout
0.1	0.0001	timeout	timeout	timeout	cand. sol./ 11.1
0.01	0.001	timeout	timeout	timeout	timeout
0.01	0.0001	cand. sol./ 5882.5	timeout	timeout	timeout
0.001	0.0001	timeout	timeout	timeout	timeout

Table 18. Results and runtimes for 3_finding_parameters, BMC depth 15

msw	prabs	hysat-0.8.6	isat_1.0r1322	isat_r2117	isat_sf_r2117
0.1	0.01	timeout	cand. sol./ 6288.0	timeout	cand. sol./ 2.0
0.1	0.001	timeout	timeout	timeout	cand. sol./ 3.8
0.1	0.0001	cand. sol./ 1517.2	timeout	timeout	timeout
0.01	0.001	timeout	timeout	timeout	timeout
0.01	0.0001	timeout	timeout	timeout	timeout
0.001	0.0001	timeout	timeout	timeout	timeout

Table 19. Results and runtimes for 3_finding_parameters, BMC depth 16

msw	prabs	hysat-0.8.6	isat_1.0r1322	isat_r2117	isat_sf_r2117
0.1	0.01	timeout	cand. sol./ 8126.9	timeout	cand. sol./ 2.3
0.1	0.001	timeout	timeout	timeout	timeout
0.1	0.0001	timeout	timeout	timeout	timeout
0.01	0.001	timeout	timeout	timeout	timeout
0.01	0.0001	timeout	timeout	timeout	timeout
0.001	0.0001	timeout	timeout	timeout	timeout

Table 20. Results and runtimes for 3_finding_parameters, BMC depth 17

msw	prabs	hysat-0.8.6	isat_1.0r1322	isat_r2117	isat_sf_r2117
0.1	0.01	timeout	timeout	timeout	timeout
0.1	0.001	timeout	timeout	timeout	timeout
0.1	0.0001	timeout	timeout	timeout	timeout
0.01	0.001	timeout	timeout	timeout	timeout
0.01	0.0001	timeout	timeout	timeout	timeout
0.001	0.0001	timeout	timeout	timeout	timeout

Table 21. Results and runtimes for 3_finding_parameters, BMC depth 18

3.4 Finding parameters for staying in a given fixed point (4_finding_parameters_fixed_point)

We modify the previous experiment by using the large road network again and adding an intended fixed point to the constraint system, i.e. a solution must now contain maximum flow rates such that the amount of traffic in each subcell stays constant at a pre-defined value using these rates. Additionally, flow rates must satisfy constraints relating them to each other, e.g. rates for cells along one of the axes in the model must be the same except at crossings where instead a distribution of traffic is prescribed.

We report results and runtimes for BMC depth 5 (note that depth 1 would suffice here, since a real fixed point of all subcells is requested in the model) in Table 22. Except for the coarsest parameters, for which all solvers consistently find candidate solution boxes, the formula is found unsatisfiable when finer search parameters are used. The `isat_sf_r2117` solver is an exception here: it still detects candidate solutions in two cases (with a very liberal minimum splitting width) where the other solvers have already found proofs for unsatisfiability. As the msw used is untypically wide, this does, however, not constitute a conspicuity.

msw	prabs	<code>hysat-0.8.6</code>	<code>isat_1.0r1322</code>	<code>isat_r2117</code>	<code>isat_sf_r2117</code>
0.1	0.01	cand. sol./ 20.6	cand. sol./ 51.1	cand. sol./ 43.5	cand. sol./ 68.1
0.1	0.001	unsat/ 1.7	unsat/ 9.5	unsat/ 2.3	cand. sol./ 44.8
0.1	0.0001	unsat/ 2.0	unsat/ 22.4	unsat/ 28.6	cand. sol./ 50.3
0.01	0.001	unsat/ 0.5	unsat/ 0.7	unsat/ 0.9	unsat/ 10.2
0.01	0.0001	unsat/ 2.3	unsat/ 0.7	unsat/ 1.0	unsat/ 1.4
0.001	0.0001	unsat/ 1.0	unsat/ 0.8	unsat/ 0.9	unsat/ 1.4

Table 22. Results and runtimes for finding parameters for a given fixed point, filed under `4_finding_paramerters_fixed_point`

3.5 Absence of stable regions (5_absence_of_stable_regions)

An extension to the idea underlying the first experiments is to search for regions of convergence instead of actual fixed points. In this experiment, we try to prove that within certain regions of the search space no points exist such that a trajectory starting in an ϵ -neighborhood E of this point will stay inside E for a bounded number of steps. Technically, we allow the centerpoint of E to lie within a large region R for which we expect that no stable behavior is possible. Initially, a trajectory must start within E , and then each variable instance of the BMC unwinding is constrained by the transition system to also stay inside E . If the solver then detects unsatisfiability of the formula, we know that no point exists within R , such that a trajectory stays within its ϵ -vicinity for the examined number of steps (and hence neither for any larger number). R thus does not contain an ϵ stable subregion.

Using a fixed number of unwindings $k = 5$, Tables 23 to 27 show the results and runtimes. A clear phase shift can be observed depending on the width of the stability corridor: while it is relatively easy to prove the absence of such a corridor within R for widths $\epsilon \leq 0.1$, it becomes impossible within the allocated amount of time for widths $\epsilon \geq 0.15$.

3.6 Bounded containment in regions (6_bounded_stable_regions)

In this experiment, we aim at detecting trajectories that start from a given region A with small width ϵ_i and leave a wider corridor B around that region with width ϵ_f . Conversely, if no such trajectory is found, this proves that all trajectories starting from A will not leave B within the given number of steps. The proof obligation can thus be seen as another type of stability proof — weaker but of potential practical interest, e.g. for detecting for how long an achieved desired situation will be kept stable before finally being left again.

msw	prabs	hysat-0.8.6	isat_1.0r1322	isat_r2117	isat_sf_r2117
0.1	0.01	unsat/ 0.4	unsat/ 0.7	unsat/ 1.1	unsat/ 0.4
0.1	0.001	unsat/ 0.7	unsat/ 0.7	unsat/ 1.2	unsat/ 0.7
0.1	0.0001	unsat/ 0.8	unsat/ 0.7	unsat/ 1.3	unsat/ 0.7
0.01	0.001	unsat/ 0.4	unsat/ 1.2	unsat/ 2.5	unsat/ 0.6
0.01	0.0001	unsat/ 1.2	unsat/ 1.5	unsat/ 3.2	unsat/ 0.6
0.001	0.0001	unsat/ 1.2	unsat/ 2.2	unsat/ 2.1	unsat/ 0.5

Table 23. Results and runtimes for 5_absence_of_stable_regions with $\epsilon = 0.01$

msw	prabs	hysat-0.8.6	isat_1.0r1322	isat_r2117	isat_sf_r2117
0.1	0.01	unsat/ 0.8	unsat/ 1.0	unsat/ 3.1	unsat/ 0.9
0.1	0.001	unsat/ 0.9	unsat/ 2.1	unsat/ 3.1	unsat/ 1.7
0.1	0.0001	unsat/ 1.2	unsat/ 1.4	unsat/ 2.3	unsat/ 1.9
0.01	0.001	unsat/ 1.1	unsat/ 3.0	unsat/ 12.3	unsat/ 1.0
0.01	0.0001	unsat/ 1.7	unsat/ 2.5	unsat/ 2.8	unsat/ 1.4
0.001	0.0001	unsat/ 1.4	unsat/ 2.6	unsat/ 3.1	unsat/ 1.5

Table 24. Results and runtimes for 5_absence_of_stable_regions with $\epsilon = 0.05$

msw	prabs	hysat-0.8.6	isat_1.0r1322	isat_r2117	isat_sf_r2117
0.1	0.01	unsat/ 70.3	unsat/ 239.9	timeout	unsat/ 2954.6
0.1	0.001	unsat/ 9.1	unsat/ 334.4	unsat/ 40.0	unsat/ 252.4
0.1	0.0001	unsat/ 26.8	unsat/ 373.2	unsat/ 308.6	unsat/ 432.2
0.01	0.001	unsat/ 6.9	unsat/ 73.6	unsat/ 2352.2	unsat/ 504.8
0.01	0.0001	unsat/ 14.3	unsat/ 137.8	unsat/ 137.1	unsat/ 20.3
0.001	0.0001	unsat/ 16.5	unsat/ 217.7	unsat/ 4368.7	unsat/ 20.8

Table 25. Results and runtimes for 5_absence_of_stable_regions with $\epsilon = 0.1$

msw	prabs	hysat-0.8.6	isat_1.0r1322	isat_r2117	isat_sf_r2117
0.1	0.01	timeout	timeout	timeout	timeout
0.1	0.001	timeout	timeout	timeout	timeout
0.1	0.0001	timeout	timeout	timeout	timeout
0.01	0.001	timeout	timeout	timeout	timeout
0.01	0.0001	timeout	timeout	timeout	timeout
0.001	0.0001	timeout	timeout	timeout	timeout

Table 26. Results and runtimes for 5_absence_of_stable_regions with $\epsilon = 0.15$

msw	prabs	hysat-0.8.6	isat_1.0r1322	isat_r2117	isat_sf_r2117
0.1	0.01	timeout	timeout	timeout	timeout
0.1	0.001	timeout	timeout	timeout	timeout
0.1	0.0001	timeout	timeout	timeout	timeout
0.01	0.001	timeout	timeout	timeout	timeout
0.01	0.0001	timeout	timeout	timeout	timeout
0.001	0.0001	timeout	timeout	timeout	timeout

Table 27. Results and runtimes for 5_absence_of_stable_regions with $\epsilon = 0.3$

Tables 28 to 32 show the results for different corridor widths. Clearly observable is that for the very tight initial corridor, relatively large numbers of unwindings can be proven to contain the trajectories within the wider corridor. In these cases, the last unwinding depths contribute already significant parts of the overall runtime such that it cannot be expected to reach much longer unwindings without investing substantially more time. For the larger ϵ_i values, i.e. wider initial corridors, reaching the outer border — which is much closer to the inner region — is simpler, and the solvers hence find trajectories leaving this region even for low numbers of unwindings.

3.7 Unbounded containment in regions (7_unbounded_region_stability)

A successful proof obtained in the previous experiment only provides an argument for a bounded number of unwindings. After one step, the trajectory may be anywhere in the wider corridor. In the last experiment we therefore tried to prove that trajectories will eventually come back to the initial corridor — thereby allowing inductive reasoning to show that they will infinitely often be in the inner corridor, and if sufficiently many depths can be shown to satisfy the property, even allowing to show that trajectories will eventually stay within the region forever after an initial don't-care phase. This property has been coined region stability in [6]. The rationale underlying the inductive proof rule used here is explained in [1].

We therefore use the same region as initial and final corridor and look for trajectories starting in that region and lying outside after an increasing number of steps. If for a depth k no such trajectory is found, proving unsatisfiability for the successive $k - 1$ depths would suffice to prove that all trajectories can leave the initial region for at most $k - 1$ steps at the beginning and then stay inside.

Tables 33 to 52 summarize results and runtimes for this experiment. Unfortunately, our solvers could not find any unsatisfiable instance for one of the settings within the first 10 unwindings, yet a number of candidate solutions. The latter might indicate that the tried region was actually inadequate or that 10 steps were simply insufficient for the system to stabilize safely into the region.

4 Conclusions

In this report, we have shown that iSAT [2] can handle some verification conditions for road networks that are well beyond the scope of numerical simulation, like finding fixed points of traffic flows or excluding existence of fixed points outside certain regions. As such fixed points represent stable operational conditions of the road network, corresponding to constant flow of traffic, they are of imminent importance to traffic engineers. Mechanized means of finding such fixed points — or, even more important in practice, finding almost-fixed points stable up to a given tolerance — as well as identifying regions of absence of such stable operational points are thus highly desirable. Our experiments show that iSAT provides the algorithmic ingredients facilitating such procedures — without, however, reaching the level of scalability that would be needed in practice to deal with major road networks. Some techniques alleviating the scalability issues will be addressed in AVACS Phase 3, while others would have to exploit special structures of the traffic-flow problem and are thus beyond scope of AVACS, which deals with general-purpose solvers. Examples of such problem-specific optimizations, which are to be deferred to focussed, application-oriented projects, are dedicated techniques exploiting conservation of mass, monotonicity (or antitonicity) of flows in source and target saturation, and the like. All these properties offer prospects of additional inference rules redundantizing whole trees of decisions and long deduction chains in iSAT. Unfortunately, they are absolutely domain-specific and are thus not in the focus of AVACS.

In Phase 3, AVACS project H1/2 will however address the problem of synergy between simulation and systematic search in constraint solving. We will integrate the idea of statistical hypothesis testing based on sampled simulated trajectories into the systematic search algorithm of iSAT. This provides an informed guiding mechanism for iSAT's search procedure that combines the benefits of both statistical model-checking and systematic search, targeting confidence levels well beyond

msw	prabs	k	hysat-0.8.6	isat_1.0r1322	isat_r2117	isat_sf_r2117
0.1	0.01	1	unsat/ 0.0	unsat/ 0.0	unsat/ 0.0	unsat/ 0.0
0.1	0.01	2	unsat/ 0.0	unsat/ 0.0	unsat/ 0.0	unsat/ 0.0
0.1	0.01	3	unsat/ 0.0	unsat/ 0.0	unsat/ 0.0	unsat/ 0.0
0.1	0.01	4	unsat/ 0.1	unsat/ 0.3	unsat/ 0.5	unsat/ 0.6
0.1	0.01	5	unsat/ 8.7	unsat/ 38.5	unsat/ 30.1	unsat/ 142.3
0.1	0.01	6	unsat/ 633.9	unsat/ 6458.0	unsat/ 8978.6	timeout
0.1	0.01	7	timeout	timeout	timeout	
0.1	0.001	1	unsat/ 0.0	unsat/ 0.0	unsat/ 0.0	unsat/ 0.0
0.1	0.001	2	unsat/ 0.0	unsat/ 0.0	unsat/ 0.0	unsat/ 0.0
0.1	0.001	3	unsat/ 0.0	unsat/ 0.0	unsat/ 0.0	unsat/ 0.0
0.1	0.001	4	unsat/ 0.2	unsat/ 0.5	unsat/ 0.6	unsat/ 0.5
0.1	0.001	5	unsat/ 8.3	unsat/ 10.8	unsat/ 15.0	unsat/ 60.9
0.1	0.001	6	unsat/ 1114.5	unsat/ 2615.3	unsat/ 6010.1	timeout
0.1	0.001	7	timeout	timeout	timeout	
0.1	0.0001	1	unsat/ 0.0	unsat/ 0.0	unsat/ 0.0	unsat/ 0.0
0.1	0.0001	2	unsat/ 0.0	unsat/ 0.0	unsat/ 0.0	unsat/ 0.0
0.1	0.0001	3	unsat/ 0.0	unsat/ 0.0	unsat/ 0.0	unsat/ 0.0
0.1	0.0001	4	unsat/ 0.2	unsat/ 0.9	unsat/ 0.6	unsat/ 0.9
0.1	0.0001	5	unsat/ 21.2	unsat/ 11.1	unsat/ 8.6	unsat/ 55.2
0.1	0.0001	6	unsat/ 2394.6	unsat/ 1480.4	unsat/ 2398.0	timeout
0.1	0.0001	7	timeout	timeout	timeout	
0.01	0.001	1	unsat/ 0.0	unsat/ 0.0	unsat/ 0.0	unsat/ 0.0
0.01	0.001	2	unsat/ 0.0	unsat/ 0.0	unsat/ 0.0	unsat/ 0.0
0.01	0.001	3	unsat/ 0.0	unsat/ 0.0	unsat/ 0.1	unsat/ 0.0
0.01	0.001	4	unsat/ 0.4	unsat/ 0.8	unsat/ 0.9	unsat/ 0.6
0.01	0.001	5	unsat/ 10.5	unsat/ 20.7	unsat/ 29.7	unsat/ 27.2
0.01	0.001	6	unsat/ 252.7	unsat/ 411.9	unsat/ 649.0	unsat/ 6381.4
0.01	0.001	7	unsat/ 1688.3	unsat/ 8114.4	timeout	timeout
0.01	0.001	8	timeout	timeout		
0.001	0.0001	1	unsat/ 0.0	unsat/ 0.0	unsat/ 0.0	unsat/ 0.0
0.001	0.0001	2	unsat/ 0.0	unsat/ 0.0	unsat/ 0.0	unsat/ 0.0
0.001	0.0001	3	unsat/ 0.0	unsat/ 0.0	unsat/ 0.1	unsat/ 0.1
0.001	0.0001	4	unsat/ 0.3	unsat/ 0.9	unsat/ 1.0	unsat/ 0.4
0.001	0.0001	5	unsat/ 15.9	unsat/ 10.0	unsat/ 14.4	unsat/ 67.7
0.001	0.0001	6	unsat/ 163.8	unsat/ 1552.3	unsat/ 810.2	timeout
0.001	0.0001	7	timeout	timeout	timeout	
0.0001	0.0001	1	unsat/ 0.0	unsat/ 0.0	unsat/ 0.0	unsat/ 0.0
0.0001	0.0001	2	unsat/ 0.0	unsat/ 0.0	unsat/ 0.0	unsat/ 0.0
0.0001	0.0001	3	unsat/ 0.0	unsat/ 0.0	unsat/ 0.1	unsat/ 0.1
0.0001	0.0001	4	unsat/ 0.6	unsat/ 0.4	unsat/ 1.5	unsat/ 2.0
0.0001	0.0001	5	unsat/ 21.4	unsat/ 22.5	unsat/ 53.4	unsat/ 114.3
0.0001	0.0001	6	unsat/ 201.6	unsat/ 2305.4	unsat/ 3711.9	timeout
0.0001	0.0001	7	unsat/ 2126.7	timeout	timeout	
0.0001	0.0001	8	timeout			

Table 28. Results for depth k and cumulative runtimes (up to k) for `6_bounded_stable_regions`, initial corridor width $\epsilon_i = 0.05$, final corridor width $\epsilon_f = 1.0$

msw	prabs	k	hysat-0.8.6	isat_1.0r1322	isat_r2117	isat_sf_r2117
0.1	0.01	1	unsat/ 0.0	unsat/ 0.0	unsat/ 0.0	unsat/ 0.0
0.1	0.01	2	unsat/ 0.0	unsat/ 0.0	unsat/ 0.0	unsat/ 0.0
0.1	0.01	3	unsat/ 0.2	unsat/ 0.2	unsat/ 0.5	unsat/ 0.4
0.1	0.01	4	unsat/ 31.6	unsat/ 7.8	unsat/ 24.5	unsat/ 222.1
0.1	0.01	5	unsat/ 2078.9	unsat/ 7593.1	unsat/ 3661.3	timeout
0.1	0.01	6	timeout	timeout	timeout	
0.1	0.001	1	unsat/ 0.0	unsat/ 0.0	unsat/ 0.0	unsat/ 0.0
0.1	0.001	2	unsat/ 0.0	unsat/ 0.0	unsat/ 0.0	unsat/ 0.0
0.1	0.001	3	unsat/ 0.3	unsat/ 0.3	unsat/ 0.3	unsat/ 0.4
0.1	0.001	4	unsat/ 13.8	unsat/ 39.2	unsat/ 43.7	unsat/ 185.6
0.1	0.001	5	unsat/ 4790.6	unsat/ 7330.0	timeout	timeout
0.1	0.001	6	timeout	timeout		
0.1	0.0001	1	unsat/ 0.0	unsat/ 0.0	unsat/ 0.0	unsat/ 0.0
0.1	0.0001	2	unsat/ 0.0	unsat/ 0.0	unsat/ 0.0	unsat/ 0.0
0.1	0.0001	3	unsat/ 0.3	unsat/ 0.8	unsat/ 0.4	unsat/ 0.5
0.1	0.0001	4	unsat/ 9.8	unsat/ 18.9	unsat/ 30.5	unsat/ 103.6
0.1	0.0001	5	unsat/ 2911.5	unsat/ 6433.4	unsat/ 1022.1	timeout
0.1	0.0001	6	timeout	timeout	timeout	
0.01	0.001	1	unsat/ 0.0	unsat/ 0.0	unsat/ 0.0	unsat/ 0.0
0.01	0.001	2	unsat/ 0.0	unsat/ 0.0	unsat/ 0.0	unsat/ 0.0
0.01	0.001	3	unsat/ 0.5	unsat/ 0.3	unsat/ 0.6	unsat/ 1.5
0.01	0.001	4	unsat/ 28.8	unsat/ 53.0	unsat/ 34.7	unsat/ 444.0
0.01	0.001	5	unsat/ 1485.6	unsat/ 3391.6	unsat/ 7231.5	timeout
0.01	0.001	6	timeout	timeout	timeout	
0.001	0.0001	1	unsat/ 0.0	unsat/ 0.0	unsat/ 0.0	unsat/ 0.0
0.001	0.0001	2	unsat/ 0.0	unsat/ 0.0	unsat/ 0.0	unsat/ 0.0
0.001	0.0001	3	unsat/ 0.4	unsat/ 0.4	unsat/ 1.1	unsat/ 1.0
0.001	0.0001	4	unsat/ 11.8	unsat/ 97.2	unsat/ 44.1	unsat/ 405.1
0.001	0.0001	5	unsat/ 451.1	unsat/ 3747.8	unsat/ 1871.2	timeout
0.001	0.0001	6	timeout	timeout	timeout	
0.0001	0.0001	1	unsat/ 0.0	unsat/ 0.0	unsat/ 0.0	unsat/ 0.0
0.0001	0.0001	2	unsat/ 0.0	unsat/ 0.0	unsat/ 0.0	unsat/ 0.0
0.0001	0.0001	3	unsat/ 0.5	unsat/ 1.1	unsat/ 0.6	unsat/ 1.2
0.0001	0.0001	4	unsat/ 30.1	unsat/ 27.2	unsat/ 35.8	unsat/ 386.4
0.0001	0.0001	5	unsat/ 606.3	unsat/ 4374.7	unsat/ 4534.0	timeout
0.0001	0.0001	6	timeout	timeout	timeout	

Table 29. Results for depth k and cumulative runtimes (up to k) for `6_bounded_stable_regions`, initial corridor width $\epsilon_i = 0.1$, final corridor width $\epsilon_f = 1.0$

msw	prabs	k	hysat-0.8.6	isat_1.0r1322	isat_r2117	isat_sf_r2117
0.1	0.01	1	unsat/ 0.0	unsat/ 0.0	unsat/ 0.0	unsat/ 0.0
0.1	0.01	2	cand. sol./ 0.9	cand. sol./ 1.0	unsat/ 2.2	cand. sol./ 0.7
0.1	0.01	3	cand. sol./ 96.7		cand. sol./ 170.4	
0.1	0.001	1	unsat/ 0.0	unsat/ 0.0	unsat/ 0.0	unsat/ 0.0
0.1	0.001	2	cand. sol./ 0.4	unsat/ 2.0	cand. sol./ 1.0	cand. sol./ 1.0
0.1	0.001	3	cand. sol./ 478.8	unsat/ 2310.6		
0.1	0.001	4	timeout	timeout		
0.1	0.0001	1	unsat/ 0.0	unsat/ 0.0	unsat/ 0.1	unsat/ 0.0
0.1	0.0001	2	cand. sol./ 1.1	unsat/ 3.5	unsat/ 5.6	cand. sol./ 2.2
0.1	0.0001	3	cand. sol./ 3653.8	unsat/ 1293.2	cand. sol./ 257.7	
0.1	0.0001	4	timeout	timeout		
0.01	0.001	1	unsat/ 0.0	unsat/ 0.0	unsat/ 0.0	unsat/ 0.0
0.01	0.001	2	unsat/ 24.0	unsat/ 2.4	unsat/ 2.3	unsat/ 41.4
0.01	0.001	3	unsat/ 9838.5	unsat/ 1143.4	unsat/ 4271.7	timeout
0.01	0.001	4	timeout	timeout	timeout	
0.01	0.0001	1	unsat/ 0.0	unsat/ 0.0	unsat/ 0.0	unsat/ 0.0
0.01	0.0001	2	unsat/ 20.1	unsat/ 3.3	unsat/ 2.9	unsat/ 29.8
0.01	0.0001	3	unsat/ 6178.5	unsat/ 847.7	unsat/ 1959.7	timeout
0.01	0.0001	4	timeout	timeout	timeout	
0.001	0.0001	1	unsat/ 0.0	unsat/ 0.0	unsat/ 0.1	unsat/ 0.0
0.001	0.0001	2	unsat/ 27.0	unsat/ 3.6	unsat/ 4.4	unsat/ 30.4
0.001	0.0001	3	timeout	unsat/ 1226.6	unsat/ 1248.5	timeout
0.001	0.0001	4		timeout	timeout	

Table 30. Results for depth k and cumulative runtimes (up to k) for `6_bounded_stable_regions`, initial corridor width $\epsilon_i = 0.3$, final corridor width $\epsilon_f = 1.0$

msw	prabs	k	hysat-0.8.6	isat_1.0r1322	isat_r2117	isat_sf_r2117
0.1	0.01	1	cand. sol./ 0.0	cand. sol./ 0.1	cand. sol./ 0.0	cand. sol./ 0.1
0.1	0.001	1	cand. sol./ 0.0	cand. sol./ 0.0	cand. sol./ 0.0	cand. sol./ 0.1
0.1	0.0001	1	cand. sol./ 0.0	cand. sol./ 0.0	cand. sol./ 0.0	cand. sol./ 0.1
0.01	0.001	1	cand. sol./ 0.0	cand. sol./ 0.1	cand. sol./ 0.0	cand. sol./ 0.8
0.01	0.0001	1	cand. sol./ 0.4	cand. sol./ 0.1	cand. sol./ 0.0	cand. sol./ 0.1
0.001	0.0001	1	cand. sol./ 0.1	cand. sol./ 0.1	cand. sol./ 0.1	cand. sol./ 0.2

Table 31. Results for depth k and cumulative runtimes (up to k) for `6_bounded_stable_regions`, initial corridor width $\epsilon_i = 0.5$, final corridor width $\epsilon_f = 1.0$

msw	prabs	k	hysat-0.8.6	isat_1.0r1322	isat_r2117	isat_sf_r2117
0.1	0.01	1	cand. sol./ 0.0	cand. sol./ 0.1	cand. sol./ 0.0	cand. sol./ 0.2
0.1	0.001	1	cand. sol./ 0.0	cand. sol./ 0.1	cand. sol./ 0.0	cand. sol./ 0.3
0.1	0.0001	1	cand. sol./ 0.0	cand. sol./ 0.1	cand. sol./ 0.1	cand. sol./ 0.1
0.01	0.001	1	cand. sol./ 0.1	cand. sol./ 0.1	cand. sol./ 0.0	cand. sol./ 1.9
0.01	0.0001	1	cand. sol./ 0.3	cand. sol./ 0.2	cand. sol./ 0.0	cand. sol./ 0.3
0.001	0.0001	1	cand. sol./ 0.3	cand. sol./ 0.2	cand. sol./ 0.1	cand. sol./ 0.4

Table 32. Results for depth k and cumulative runtimes (up to k) for `6_bounded_stable_regions`, initial corridor width $\epsilon_i = 0.8$, final corridor width $\epsilon_f = 1.0$

msw	prabs	hysat-0.8.6	isat_1.0r1322	isat_r2117	isat_sf_r2117
0.1	0.01	cand. sol./ 0.0	cand. sol./ 0.0	cand. sol./ 0.0	cand. sol./ 0.0
0.1	0.001	cand. sol./ 0.0	cand. sol./ 0.0	cand. sol./ 0.0	cand. sol./ 0.1
0.1	0.0001	cand. sol./ 0.0	cand. sol./ 0.0	cand. sol./ 0.1	cand. sol./ 0.1
0.01	0.001	cand. sol./ 0.1	cand. sol./ 0.0	cand. sol./ 0.0	cand. sol./ 0.1
0.01	0.0001	cand. sol./ 0.1	cand. sol./ 0.1	cand. sol./ 0.2	cand. sol./ 0.1
0.001	0.0001	cand. sol./ 0.1	cand. sol./ 0.1	cand. sol./ 0.1	cand. sol./ 0.1

Table 33. Results and runtimes for `7_unbounded_region_stability`, $\epsilon = 0.5$, BMC depth 1

msw	prabs	hysat-0.8.6	isat_1.0r1322	isat_r2117	isat_sf_r2117
0.1	0.01	cand. sol./ 0.0	cand. sol./ 0.0	cand. sol./ 0.2	cand. sol./ 0.4
0.1	0.001	cand. sol./ 0.1	cand. sol./ 0.0	cand. sol./ 0.1	cand. sol./ 0.2
0.1	0.0001	cand. sol./ 5.9	cand. sol./ 0.0	cand. sol./ 0.1	cand. sol./ 0.4
0.01	0.001	cand. sol./ 0.3	cand. sol./ 0.2	cand. sol./ 0.6	cand. sol./ 1.6
0.01	0.0001	cand. sol./ 2.3	cand. sol./ 0.2	cand. sol./ 1.1	cand. sol./ 19.4
0.001	0.0001	cand. sol./ 0.8	cand. sol./ 1.6	cand. sol./ 1.6	cand. sol./ 0.5

Table 34. Results and runtimes for `7_unbounded_region_stability`, $\epsilon = 0.5$, BMC depth 2

msw	prabs	hysat-0.8.6	isat_1.0r1322	isat_r2117	isat_sf_r2117
0.1	0.01	cand. sol./ 0.1	cand. sol./ 0.9	cand. sol./ 0.1	cand. sol./ 0.5
0.1	0.001	cand. sol./ 0.4	cand. sol./ 2.5	cand. sol./ 8.9	cand. sol./ 8.9
0.1	0.0001	cand. sol./ 0.7	cand. sol./ 0.1	cand. sol./ 1.5	cand. sol./ 7.0
0.01	0.001	cand. sol./ 3.3	cand. sol./ 2.7	cand. sol./ 42.1	cand. sol./ 2.3
0.01	0.0001	cand. sol./ 35.3	cand. sol./ 19.5	cand. sol./ 109.0	cand. sol./ 6.3
0.001	0.0001	cand. sol./ 27.4	cand. sol./ 57.6	cand. sol./ 6.8	cand. sol./ 76.1

Table 35. Results and runtimes for `7_unbounded_region_stability`, $\epsilon = 0.5$, BMC depth 3

msw	prabs	hysat-0.8.6	isat_1.0r1322	isat_r2117	isat_sf_r2117
0.1	0.01	cand. sol./ 0.4	cand. sol./ 0.4	cand. sol./ 3.0	cand. sol./ 1.8
0.1	0.001	cand. sol./ 8.9	cand. sol./ 5.0	cand. sol./ 12.2	cand. sol./ 249.6
0.1	0.0001	cand. sol./ 12.1	cand. sol./ 9.7	cand. sol./ 6.8	cand. sol./ 13.5
0.01	0.001	cand. sol./ 48.6	cand. sol./ 166.4	cand. sol./ 433.8	cand. sol./ 55.2
0.01	0.0001	cand. sol./ 31.2	cand. sol./ 2054.4	cand. sol./ 49.5	cand. sol./ 415.8
0.001	0.0001	cand. sol./ 1066.8	timeout	cand. sol./ 24.4	cand. sol./ 1480.9

Table 36. Results and runtimes for `7_unbounded_region_stability`, $\epsilon = 0.5$, BMC depth 4

msw	prabs	hysat-0.8.6	isat_1.0r1322	isat_r2117	isat_sf_r2117
0.1	0.01	cand. sol./ 0.1	cand. sol./ 4.7	cand. sol./ 0.7	cand. sol./ 24.8
0.1	0.001	cand. sol./ 17.7	cand. sol./ 191.3	cand. sol./ 21.3	cand. sol./ 20.6
0.1	0.0001	cand. sol./ 39.0	cand. sol./ 215.7	cand. sol./ 7.9	cand. sol./ 3.5
0.01	0.001	cand. sol./ 24.0	cand. sol./ 4900.1	timeout	timeout
0.01	0.0001	cand. sol./ 172.7	timeout	cand. sol./ 3236.1	timeout
0.001	0.0001	cand. sol./ 46.0	timeout	cand. sol./ 537.2	timeout

Table 37. Results and runtimes for `7_unbounded_region_stability`, $\epsilon = 0.5$, BMC depth 5

msw	prabs	hysat-0.8.6	isat_1.0r1322	isat_r2117	isat_sf_r2117
0.1	0.01	cand. sol./ 9.0	cand. sol./ 57.9	cand. sol./ 6.6	cand. sol./ 5.7
0.1	0.001	cand. sol./ 11.0	cand. sol./ 26.6	cand. sol./ 10.9	cand. sol./ 25.1
0.1	0.0001	cand. sol./ 66.9	cand. sol./ 145.3	cand. sol./ 147.1	cand. sol./ 3924.7
0.01	0.001	cand. sol./ 912.8	timeout	timeout	cand. sol./ 202.8
0.01	0.0001	cand. sol./ 214.1	cand. sol./ 4424.0	timeout	cand. sol./ 505.7
0.001	0.0001	timeout	timeout	cand. sol./ 295.2	timeout

Table 38. Results and runtimes for `7_unbounded_region_stability`, $\epsilon = 0.5$, BMC depth 6

msw	prabs	hysat-0.8.6	isat_1.0r1322	isat_r2117	isat_sf_r2117
0.1	0.01	cand. sol./ 3.2	cand. sol./ 1.2	cand. sol./ 33.6	cand. sol./ 40.0
0.1	0.001	cand. sol./ 139.1	cand. sol./ 344.2	cand. sol./ 1270.8	cand. sol./ 7972.4
0.1	0.0001	cand. sol./ 12.7	cand. sol./ 1958.0	cand. sol./ 73.8	cand. sol./ 60.9
0.01	0.001	cand. sol./ 8256.1	cand. sol./ 739.9	timeout	timeout
0.01	0.0001	cand. sol./ 769.7	timeout	timeout	timeout
0.001	0.0001	timeout	cand. sol./ 8319.8	timeout	timeout

Table 39. Results and runtimes for `7_unbounded_region_stability`, $\epsilon = 0.5$, BMC depth 7

msw	prabs	hysat-0.8.6	isat_1.0r1322	isat_r2117	isat_sf_r2117
0.1	0.01	cand. sol./ 3.6	cand. sol./ 46.4	cand. sol./ 21.2	cand. sol./ 105.9
0.1	0.001	cand. sol./ 2571.9	timeout	timeout	timeout
0.1	0.0001	cand. sol./ 5791.0	timeout	cand. sol./ 7209.8	cand. sol./ 281.5
0.01	0.001	cand. sol./ 3560.4	timeout	timeout	timeout
0.01	0.0001	timeout	timeout	timeout	timeout
0.001	0.0001	timeout	timeout	timeout	timeout

Table 40. Results and runtimes for `7_unbounded_region_stability`, $\epsilon = 0.5$, BMC depth 8

msw	prabs	hysat-0.8.6	isat_1.0r1322	isat_r2117	isat_sf_r2117
0.1	0.01	cand. sol./ 10.5	cand. sol./ 17.0	cand. sol./ 386.2	cand. sol./ 4199.4
0.1	0.001	cand. sol./ 25.4	cand. sol./ 3692.7	timeout	cand. sol./ 64.6
0.1	0.0001	cand. sol./ 51.6	timeout	timeout	cand. sol./ 910.7
0.01	0.001	timeout	timeout	timeout	timeout
0.01	0.0001	timeout	timeout	timeout	timeout
0.001	0.0001	timeout	timeout	cand. sol./ 1337.9	timeout

Table 41. Results and runtimes for `7_unbounded_region_stability`, $\epsilon = 0.5$, BMC depth 9

msw	prabs	hysat-0.8.6	isat_1.0r1322	isat_r2117	isat_sf_r2117
0.1	0.01	cand. sol./ 56.8	cand. sol./ 191.8	cand. sol./ 64.9	cand. sol./ 2890.8
0.1	0.001	cand. sol./ 450.3	timeout	cand. sol./ 146.7	timeout
0.1	0.0001	cand. sol./ 147.9	timeout	timeout	cand. sol./ 46.8
0.01	0.001	timeout	timeout	timeout	timeout
0.01	0.0001	timeout	timeout	timeout	timeout
0.001	0.0001	timeout	timeout	timeout	timeout

Table 42. Results and runtimes for `7_unbounded_region_stability`, $\epsilon = 0.5$, BMC depth 10

msw	prabs	hysat-0.8.6	isat_1.0r1322	isat_r2117	isat_sf_r2117
0.1	0.01	cand. sol./ 0.0	cand. sol./ 0.0	cand. sol./ 0.0	cand. sol./ 0.2
0.1	0.001	cand. sol./ 0.0	cand. sol./ 0.0	cand. sol./ 0.0	cand. sol./ 0.3
0.1	0.0001	cand. sol./ 0.0	cand. sol./ 0.0	cand. sol./ 0.0	cand. sol./ 0.1
0.01	0.001	cand. sol./ 0.1	cand. sol./ 0.0	cand. sol./ 0.0	cand. sol./ 0.5
0.01	0.0001	cand. sol./ 0.2	cand. sol./ 0.0	cand. sol./ 0.0	cand. sol./ 0.5
0.001	0.0001	cand. sol./ 0.0	cand. sol./ 0.1	cand. sol./ 0.1	cand. sol./ 1.4

Table 43. Results and runtimes for `7_unbounded_region_stability`, $\epsilon = 0.8$, BMC depth 1

msw	prabs	hysat-0.8.6	isat_1.0r1322	isat_r2117	isat_sf_r2117
0.1	0.01	cand. sol./ 0.1	cand. sol./ 0.1	cand. sol./ 0.2	cand. sol./ 0.5
0.1	0.001	cand. sol./ 1.7	cand. sol./ 0.6	cand. sol./ 0.2	cand. sol./ 0.5
0.1	0.0001	cand. sol./ 0.2	cand. sol./ 0.4	cand. sol./ 0.2	cand. sol./ 2.8
0.01	0.001	cand. sol./ 0.6	cand. sol./ 0.2	cand. sol./ 0.5	cand. sol./ 3.1
0.01	0.0001	cand. sol./ 0.4	cand. sol./ 0.2	cand. sol./ 0.2	cand. sol./ 129.4
0.001	0.0001	cand. sol./ 0.7	cand. sol./ 19.7	cand. sol./ 1.5	cand. sol./ 1.2

Table 44. Results and runtimes for `7_unbounded_region_stability`, $\epsilon = 0.8$, BMC depth 2

msw	prabs	hysat-0.8.6	isat_1.0r1322	isat_r2117	isat_sf_r2117
0.1	0.01	cand. sol./ 0.4	cand. sol./ 0.7	cand. sol./ 1.4	cand. sol./ 0.9
0.1	0.001	cand. sol./ 0.5	cand. sol./ 1.1	cand. sol./ 0.3	cand. sol./ 7.2
0.1	0.0001	cand. sol./ 0.5	cand. sol./ 8.2	cand. sol./ 0.3	cand. sol./ 8.0
0.01	0.001	cand. sol./ 0.6	cand. sol./ 251.4	cand. sol./ 2.2	cand. sol./ 0.5
0.01	0.0001	cand. sol./ 3.8	cand. sol./ 34.2	cand. sol./ 31.5	cand. sol./ 2.4
0.001	0.0001	cand. sol./ 76.7	cand. sol./ 130.4	cand. sol./ 6.2	cand. sol./ 35.7

Table 45. Results and runtimes for `7_unbounded_region_stability`, $\epsilon = 0.8$, BMC depth 3

msw	prabs	hysat-0.8.6	isat_1.0r1322	isat_r2117	isat_sf_r2117
0.1	0.01	cand. sol./ 0.9	cand. sol./ 7.1	cand. sol./ 2.3	cand. sol./ 6.3
0.1	0.001	cand. sol./ 2.3	cand. sol./ 126.8	cand. sol./ 1623.3	cand. sol./ 89.1
0.1	0.0001	cand. sol./ 4.8	cand. sol./ 3.1	cand. sol./ 85.1	cand. sol./ 4.4
0.01	0.001	cand. sol./ 711.9	cand. sol./ 793.5	cand. sol./ 25.5	cand. sol./ 40.2
0.01	0.0001	cand. sol./ 586.0	cand. sol./ 56.7	timeout	cand. sol./ 356.1
0.001	0.0001	cand. sol./ 40.4	cand. sol./ 8033.8	cand. sol./ 23.6	timeout

Table 46. Results and runtimes for `7_unbounded_region_stability`, $\epsilon = 0.8$, BMC depth 4

msw	prabs	hysat-0.8.6	isat_1.0r1322	isat_r2117	isat_sf_r2117
0.1	0.01	cand. sol./ 8.6	cand. sol./ 119.5	cand. sol./ 38.5	cand. sol./ 279.6
0.1	0.001	cand. sol./ 31.7	timeout	cand. sol./ 38.7	cand. sol./ 167.0
0.1	0.0001	cand. sol./ 159.9	cand. sol./ 30.6	cand. sol./ 349.4	cand. sol./ 1742.4
0.01	0.001	cand. sol./ 482.4	timeout	cand. sol./ 71.0	timeout
0.01	0.0001	cand. sol./ 5697.8	timeout	cand. sol./ 3238.3	cand. sol./ 515.8
0.001	0.0001	cand. sol./ 3366.1	timeout	timeout	timeout

Table 47. Results and runtimes for `7_unbounded_region_stability`, $\epsilon = 0.8$, BMC depth 5

msw	prabs	hysat-0.8.6	isat_1.0r1322	isat_r2117	isat_sf_r2117
0.1	0.01	cand. sol./ 4.8	cand. sol./ 693.1	cand. sol./ 2.8	cand. sol./ 90.1
0.1	0.001	cand. sol./ 193.7	cand. sol./ 154.8	cand. sol./ 4432.0	cand. sol./ 3.5
0.1	0.0001	cand. sol./ 82.6	cand. sol./ 89.0	cand. sol./ 662.3	cand. sol./ 477.9
0.01	0.001	cand. sol./ 3253.9	timeout	timeout	timeout
0.01	0.0001	cand. sol./ 346.4	timeout	cand. sol./ 95.8	timeout
0.001	0.0001	timeout	timeout	cand. sol./ 2815.5	timeout

Table 48. Results and runtimes for 7_unbounded_region_stability, $\epsilon = 0.8$, BMC depth 6

msw	prabs	hysat-0.8.6	isat_1.0r1322	isat_r2117	isat_sf_r2117
0.1	0.01	cand. sol./ 208.1	cand. sol./ 21.0	cand. sol./ 39.1	cand. sol./ 22.4
0.1	0.001	cand. sol./ 52.4	timeout	cand. sol./ 1771.8	cand. sol./ 7199.0
0.1	0.0001	timeout	timeout	cand. sol./ 9315.2	timeout
0.01	0.001	timeout	timeout	timeout	timeout
0.01	0.0001	timeout	cand. sol./ 561.6	timeout	timeout
0.001	0.0001	cand. sol./ 4016.5	timeout	timeout	timeout

Table 49. Results and runtimes for 7_unbounded_region_stability, $\epsilon = 0.8$, BMC depth 7

msw	prabs	hysat-0.8.6	isat_1.0r1322	isat_r2117	isat_sf_r2117
0.1	0.01	cand. sol./ 260.3	cand. sol./ 3.6	cand. sol./ 160.0	cand. sol./ 9.9
0.1	0.001	cand. sol./ 8629.5	timeout	timeout	cand. sol./ 9113.2
0.1	0.0001	timeout	timeout	timeout	timeout
0.01	0.001	timeout	timeout	timeout	timeout
0.01	0.0001	timeout	timeout	timeout	timeout
0.001	0.0001	timeout	timeout	timeout	timeout

Table 50. Results and runtimes for 7_unbounded_region_stability, $\epsilon = 0.8$, BMC depth 8

msw	prabs	hysat-0.8.6	isat_1.0r1322	isat_r2117	isat_sf_r2117
0.1	0.01	cand. sol./ 24.3	timeout	timeout	timeout
0.1	0.001	cand. sol./ 6349.7	timeout	timeout	timeout
0.1	0.0001	timeout	timeout	timeout	timeout
0.01	0.001	timeout	timeout	timeout	timeout
0.01	0.0001	timeout	timeout	timeout	timeout
0.001	0.0001	timeout	timeout	timeout	timeout

Table 51. Results and runtimes for 7_unbounded_region_stability, $\epsilon = 0.8$, BMC depth 9

msw	prabs	hysat-0.8.6	isat_1.0r1322	isat_r2117	isat_sf_r2117
0.1	0.01	cand. sol./ 6268.1	timeout	cand. sol./ 3041.0	timeout
0.1	0.001	timeout	timeout	timeout	timeout
0.1	0.0001	timeout	timeout	timeout	timeout
0.01	0.001	timeout	timeout	timeout	timeout
0.01	0.0001	timeout	timeout	timeout	timeout
0.001	0.0001	timeout	timeout	timeout	timeout

Table 52. Results and runtimes for 7_unbounded_region_stability, $\epsilon = 0.8$, BMC depth 10

the scope of statistical hypothesis testing — and thus, statistical model checking — while improving the runtime of exhaustive checking. We will redo the experiments reported herein when that integration is operational.

References

1. Eggers, A., Ramdani, N., Nedialkov, N.S., Fränzle, M.: Improving SAT modulo ODE for hybrid systems analysis by combining different enclosure methods. In: Proceedings of the Ninth International Conference on Software Engineering and Formal Methods (SEFM). LNCS, Springer (2011), to appear
2. Fränzle, M., Herde, C., Ratschan, S., Schubert, T., Teige, T.: Efficient solving of large non-linear arithmetic constraint systems with complex boolean structure. JSAT Special Issue on Constraint Programming and SAT 1, 209–236 (2007)
3. Greenshields, B.: Proc. Highway Res. Board 14 448 (1935)
4. Helbing, D.: Improved fluid-dynamic model for vehicular traffic. Phys. Rev. E 51 (1995)
5. Lighthill, M., Whitman, G.: On kinematic waves II: A theory of traffic flow on long crowded roads. Proc. Royal Soc. A 229, 317–345 (1955)
6. Podelski, A., Wagner, S.: A sound and complete proof rule for region stability of hybrid systems. In: Proceedings of the 10th Conference on Hybrid Systems: Computation and Control. Lecture Notes in Computer Science, vol. 4416, pp. 750 – 753 (2007)